Rocks in the auxin stream: Wound-induced auxin accumulation and *ERF115* expression synergistically drive stem cell regeneration

Balkan Canher[a,b], Jefri Heyman[a,b], Maria Savina[c,d], Ajay Devendran[e], Thomas Eekhout[a,b], Ilse Vercauteren[a,b], Els Prinsen[f], Rotem Matosevich[g], Jian Xu[h], Victoria Mironova[c,d], and Lieven De Veylder[a,b,1]

[a]Department of Plant Biotechnology and Bioinformatics, Ghent University, B-9052 Ghent, Belgium; [b]Center for Plant Systems Biology, VIB, B-9052 Ghent, Belgium; [c]Department for Systems Biology, Institute of Cytology and Genetics SB RAS, 630090 Novosibirsk, Russia; [d]LCT & EB, Novosibirsk State University, 630090 Novosibirsk, Russia; [e]Department of Biological Sciences and Centre for BioImaging Sciences, National University of Singapore, Singapore 117543, Singapore; [f]Integrated Molecular Plant Physiology Research, Department of Biology, University of Antwerp, 2020 Antwerp, Belgium; [g]Institute of Plant Sciences and Genetics in Agriculture, Faculty of Agriculture, The Hebrew University of Jerusalem, Rehovot 7612001, Israel; and [h]Department of Plant Systems Physiology, Institute for Water and Wetland Research, Faculty of Science, Radboud University, 6525 AJ Nijmegen, The Netherlands

Edited by Mark Estelle, University of California San Diego, La Jolla, CA, and approved May 27, 2020 (received for review April 14, 2020)

Plants are known for their outstanding capacity to recover from various wounds and injuries. However, it remains largely unknown how plants sense diverse forms of injury and canalize existing developmental processes into the execution of a correct regenerative response. Auxin, a cardinal plant hormone with morphogen-like properties, has been previously implicated in the recovery from diverse types of wounding and organ loss. Here, through a combination of cellular imaging and in silico modeling, we demonstrate that vascular stem cell death obstructs the polar auxin flux, much alike rocks in a stream, and causes it to accumulate in the endodermis. This in turn grants the endodermal cells the capacity to undergo periclinal cell division to repopulate the vascular stem cell pool. Replenishment of the vasculature by the endodermis depends on the transcription factor ERF115, a wound-inducible regulator of stem cell division. Although not the primary inducer, auxin is required to maintain *ERF115* expression. Conversely, ERF115 sensitizes cells to auxin by activating ARF5/MONOPTEROS, an auxin-responsive transcription factor involved in the global auxin response, tissue patterning, and organ formation. Together, the wound-induced auxin accumulation and *ERF115* expression grant the endodermal cells stem cell activity. Our work provides a mechanistic model for wound-induced stem cell regeneration in which ERF115 acts as a wound-inducible stem cell organizer that interprets wound-induced auxin maxima.

regeneration | auxin | ERF115 | stem cells | *Arabidopsis*

Plant growth is controlled predominantly through cell division activity in the apical zones, called the meristems. Within the core of each meristem, a subpopulation of dividing cells can be found that operate as stem cells, collectively forming the stem cell niche (SCN). Within the *Arabidopsis* root SCN is a cluster of infrequently dividing cells, the quiescent center (QC). The QC is surrounded by a single tier of stem cells that give rise to all cells within the root, composing the columella, lateral root cap, epidermis, cortex, endodermis, and vasculature (1). The QC cells are characteristically marked by the expression of the homeobox gene *WOX5*, which maintains the quiescent state and helps to keep the SCN in an undifferentiated state (2). The position of the QC is determined by a maximum in auxin, a phytohormone involved in virtually every aspect of plant development, including organ production and tissue patterning (3, 4). Along with maintaining the SCN, auxin is known as a central player governing regenerative processes, such as recovery from wounding, organ loss, and tissue damage. Chemical or genetic perturbations in auxin biosynthesis, transport, and signaling are associated with impairments in de novo root regeneration from leaf explants, regeneration after root tip excision, adventitious rooting, tissue reunion following grafting, and the ability to form callus following wounding (5–10).

The core regulators of auxin signaling belong to three protein families: F-box TRANSPORT INHIBITOR RESPONSE/AUXIN SIGNALING F-BOX PROTEIN (TIR1/AFB) auxin receptors, AUXIN/INDOLE ACETIC ACID (AUX/IAA) transcriptional repressors, and AUXIN RESPONSE FACTOR (ARF) transcription factors (TFs). In the absence of auxin, ARFs are bound by AUX/IAA proteins, repressing their activity. The presence of auxin promotes an interaction between TIR1/AFB receptors and AUX/IAA proteins that targets them for proteasome-mediated degradation. Subsequently, ARFs collectively control the expression of a multitude of downstream target genes to constitute a global auxin response (11). The ARF with perhaps the most prominent role with respect to meristem regulation and stem cell activity is ARF5/MONOPTEROS (MP), which is involved in the formation of embryonic polarity, shoot apical meristem primordia, lateral organs, and vascular tissues (12–17).

While the ultimate source of auxin in plants is local biosynthesis and metabolism, transport of auxin is essential for communication between tissues and various aspects of morphogenesis (18). The

Significance

Plants show remarkable regenerative abilities, allowing them to recover from wounds and organ loss. This regenerative capacity is controlled in part by auxin, the most promiscuous plant hormone controlling organogenesis and tissue patterning. We show that stem cell death diverges the auxin flow, much like rocks in a stream, resulting in an auxin accumulation in the tissues surrounding the wound. We demonstrate that within these tissues, wound-induced expression of the plant-specific transcription factor ERF115 works synergistically with the change in auxin accumulation, thereby specifying stem cell identity in the cells surrounding the damaged stem cells. This gain of stem cell identity drives formative divisions, allowing replacement of the lost stem cells and thus successful regeneration.

Author contributions: B.C., J.H., V.M., and L.D.V. designed research; B.C., J.H., M.S., T.E., I.V., E.P., and V.M. performed research; B.C., A.D., R.M., and J.X. contributed new reagents/analytic tools; B.C., J.H., M.S., T.E., E.P., J.X., V.M., and L.D.V. analyzed data; and B.C., V.M., and L.D.V. wrote the paper.

The authors declare no competing interest.

This article is a PNAS Direct Submission.

Data deposition: RNA-seq data have been deposited in the Gene Expression Omnibus (GEO) database (accession no. GSE139715).

[1]To whom correspondence may be addressed. Email: lieven.deveylder@psb.vib-ugent.be.

This article contains supporting information online at https://www.pnas.org/lookup/suppl/doi:10.1073/pnas.2006620117/-/DCSupplemental.

First published June 29, 2020.

combination of local auxin biosynthesis and auxin transport leads to the creation of auxin gradients, which in turn determine the positioning of new organs and maintenance of stem cell identity (19–21). In addition, rapid changes in auxin concentration, caused by environmental factors, can mediate the physiological and molecular responses of plants to external factors, such as nutrient availability, shade avoidance, wounding, and infection (9, 18, 22–27).

Although the bulk transport of auxin to distant tissues occurs passively through vascular tissues, fine-tuning and patterning are achieved by active transport. Such directional transport of auxin

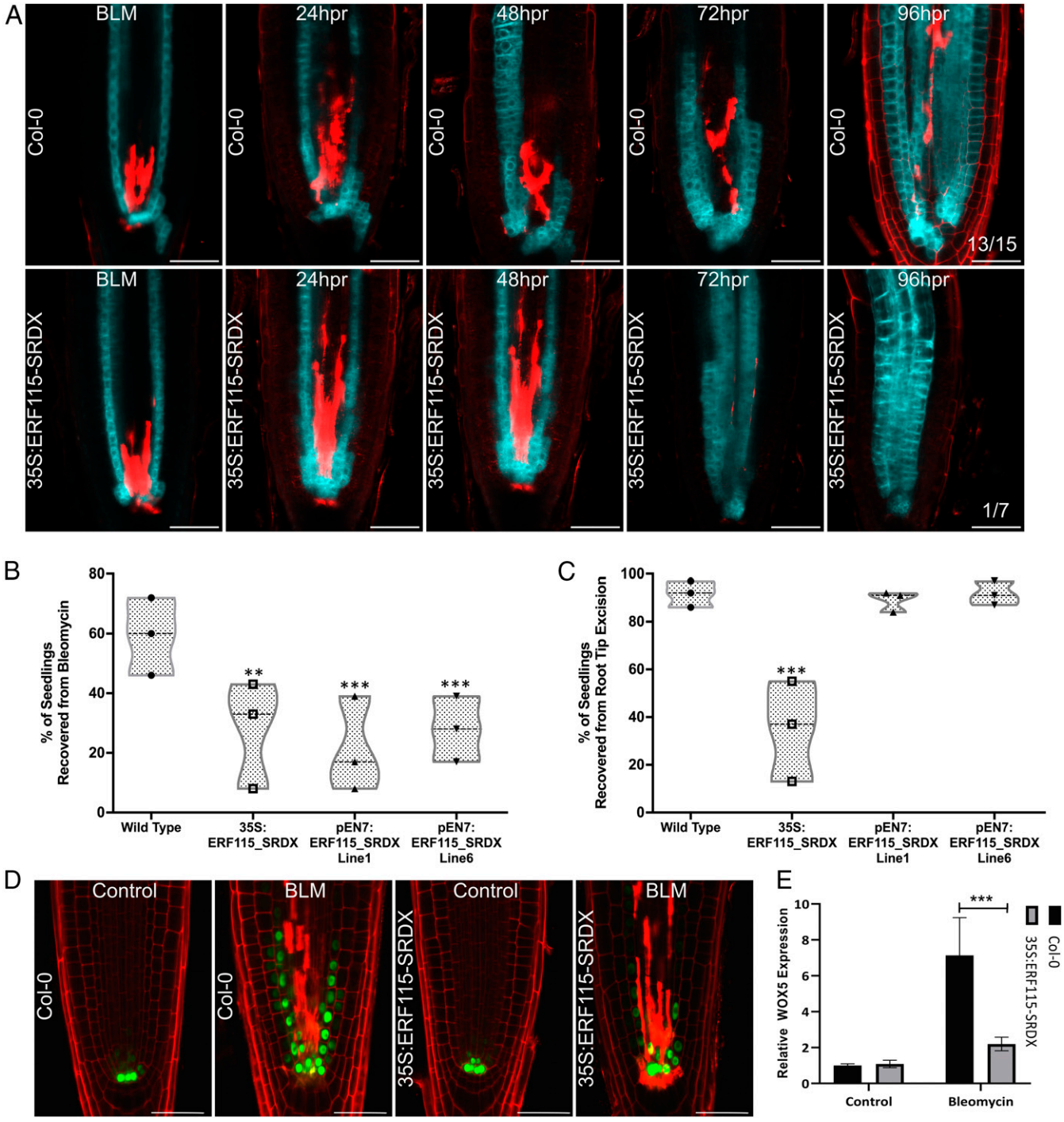

Fig. 1. (*A* and *B*) Time-lapse images of control and *pSCR:CRE-GR 35S:loxp-tOCS-loxp-CFP* seedlings in Col-0 or *35S:ERF115-SRDX* background at indicated time points: 24 h of BLM treatment or 24 to 96 h of recovery on BLM-free medium. hpr, hours postrecovery. Propidium iodide was used to stain cell walls and damaged cells. The numbers in the lower right corner indicate the number of recovered seedlings among the total number of seedlings tracked by confocal imaging. (*B* and *C*) Percentage of seedlings recovered from BLM treatment (*B*) or root tip excision (*C*). $^{**}P < 0.01$; $^{***}P < 0.001$. (*D*) *WOX5_-GFP/NLS* in the wild-type (Col-0) or *35S:ERF115-SRDX* background under control conditions or following a 24-h treatment with BLM. Propidium iodide was used as a counterstain and to stain damaged cells. (*E*) qPCR data showing relative *WOX5* expression in Col-0 and *35S:ERF115-SRDX* before or after BLM treatment. $^{***}P < 0.001$. (Scale bars in *A* and *D*: 50 μm.)

is largely mediated by efflux carrier proteins known as PINs that are polarly localized on the cell membranes (18, 28, 29). Consequently, auxin flows in a "reverse-fountain" pattern that is sustained by coordinated PIN activity and local auxin biosynthesis. The reverse-fountain pattern ensures that the auxin that travels downward through the vascular tissue cells is redirected sideways and upward after passing through the SCN and columella. Finally, it is transported back into the meristem and reinforces the auxin maximum. Through mathematical modeling, it has been demonstrated that PIN-based polar auxin transport in combination with local auxin biosynthesis is sufficient to explain such processes as vascular venation patterning, embryo axis formation, and recovery from wounding (30–32).

To obtain the plant's highly intricate tissue patterns and precisely defined cell identities, phytohormones are known to be in constant cross-talk with other molecular signaling components (33–35). ERF115, a member of the plant ethylene response factor (ERF) transcription factor family, was initially identified as a regulator of QC stem cell division (36). Aside from its role in regulating the division of slowly dividing QC stem cells, ERF115 is also a central regulator of plant regeneration responses (37). Various modes of wounding, such as mechanical removal of root meristems, DNA damage-induced stem cell death, and laser ablation, have been found to trigger a rapid transcriptional activation of *ERF115*. Expression of *ERF115* following meristematic cell death was found to be essential for the generation of new tissue files, which enables replacement of the damaged cells by new cells (37, 38). During recovery from stem cell ablation or root tip excision, ERF115 interacts with the RBR-SCR signaling network to regulate stem cell division and the response to environmental stress (39). In addition, ERF115 activity was found to be controlled through its interaction with a GRAS transcription factor, PAT1. Strikingly, co-overexpression of *ERF115-PAT1* results in hyperproliferation, triggering spontaneous callus formation (37).

Along with the identification of ERF115-interacting proteins, several studies have proposed other mechanisms to explain how cell death induces *ERF115*. A jasmonate signaling network acting in synergy with auxin was reported to cause *ERF115* induction upon wounding or nematode infection (39). Furthermore, oxygen species were shown to control the expression of *ERF115* for maintaining the stem cell division and differentiation balance (40).

Here we studied the role of ERF115 activation in endodermal cells following DNA damage-induced vascular stem cell death and its potential interplay with auxin. We found that stem cell death triggers an accumulation of auxin around the wound, due mainly to interruption of auxin transport. Although not the initial trigger for *ERF115* expression, auxin accumulation is required to sustain ERF115 activity, which confers an organizing center capacity to the endodermal cells, contributing to successful replenishment of the damaged SCN.

Results

The Endodermis Contributes Directly to Replenishment of the Vasculature in an *ERF115*-Dependent Manner. It has been previously observed that the killing of vascular cells through the administration of the DNA damage-inducing drug bleomycin (BLM) triggers the transcriptional induction of *ERF115* in QC and endodermal cells (36). *ERF115* expression was found to correlate with the occurrence of endodermal periclinal cell divisions, indicative of a role of endodermal cells in repopulating the damaged stem cell population. To visualize the contribution of the endodermal formative divisions in the replenishment of the SCN in real time, a lineage tracking tool was used to fluorescently label all endodermal cells and their daughters using a dexamethasone (DEX)-inducible *CFP* gene driven by the endodermis-specific *SCR* promoter, *pSCR:CRE_GR p35S loxp-tOCS-loxp-CFP* (23). Following induction, the CFP signal was restricted to the QC and endodermal cells in both wild type and the dominant-negative line overexpressing *ERF115* fused to the SUPERMAN REPRESSOR DOMAIN (*35S:ERF115-SRDX*) (Fig. 1*A*). In the absence of stem cell death, the CFP signal expanded only to the young cortex cells, presumably due to labeling of cortex/endodermis initials at the initial induction (*SI Appendix*, Fig. S1 *A* and *B*). In contrast, the seedlings recovering from BLM-induced vascular cell death displayed penetration of the CFP signal within the vascular bundle, indicating that the newly formed vascular cells originate from the endodermis and QC (Fig. 1*A*). However, CFP penetration was not observed in the *35S:ERF115-SRDX* background, and CFP-labeled endodermis/cortex files finally zipped together due to the collapse of the vascular bundle (Fig. 1*A*).

To determine the endodermal contribution to the replenishment of the SCN, we expressed the dominant-negative *ERF115-SRDX* fusion from the endodermis-specific *EN7* promoter. We verified that the *EN7* promoter was not ectopically induced by BLM treatment (*SI Appendix*, Fig. S1*C*). Despite showing no effect on total root elongation (*SI Appendix*, Fig. S1*E*), specific suppression of *ERF115* activity in the endodermis resulted in a substantial reduction in recovery success following BLM treatment (59% in wild type vs. 21% and 28% in two independent *EN7:ERF115-SRDX* lines) (Fig. 1*B*). The level of recovery was much like that seen in the *35S:ERF115-SRDX* line, suggesting that the endodermal cells are major contributors to the replenishment process under the tested conditions. Interestingly, in contrast to the *35S:ERF115-SRDX* line, the *EN7:ERF115-SRDX* lines displayed a recovery rate following root tip excision similar to that of wild-type plants (Fig. 1*C*), suggesting that ERF115 activity in the endodermis is not essential for recovery from root tip excision. The *erf115-1* T-DNA mutant did not differ from wild type with respect to BLM recovery performance, suggesting functional redundancy among genes closely related to *ERF115* (*SI Appendix*, Fig. S1*F*).

Wound-Induced Auxin Accumulation Grants the Endodermis at Least Partial QC Identity. It has been previously reported that on DNA damage-triggered stem cell death, genes associated with QC cell identity, such as *WOX5* and *AGL42*, become ectopically induced around the dead cells (36, 41). In accordance with these reports, we found that the expression of *WOX5* was induced upon BLM treatment (Fig. 1 *D* and *E*), suggesting a potential ectopic gain of QC identity, predominantly in the endodermis. The ectopic *WOX5* induction was strongly suppressed in the *35S:ERF115-SRDX* line, illustrating the involvement of ERF115 in attaining QC cell fate. The lack of endodermal expression of *QC25:GUS*, an independent marker of QC fate, suggests that the endodermal cells might acquire only partial QC identity following BLM treatment (*SI Appendix*, Fig. S1*D*).

We reasoned that ectopic *WOX5* expression might be indicative of a change in the auxin maximum within the root tip, and thus investigated the changes in auxin dynamics and transcriptional response during BLM recovery. After 24 h of BLM treatment, the *DR5:VENUS-NLS* reporter revealed activation of the transcriptional auxin response around and above the cell death zone, which became more pronounced after 24 h of recovery on BLM-free medium (Fig. 2*A*). We next investigated the change in auxin input using the ratiometric R2D2 reporter, for which high and low red:green ratios indicate relative high and low auxin accumulation, respectively (42). Ratiometric quantification obtained from BLM-treated R2D2 seedlings revealed that at 24 h posttreatment, auxin accumulated most pronouncedly in the vasculature and endodermal cells (Fig. 2*C* and Movies S1 and S2). These results suggest that in addition to the activation of auxin-responsive genes, as indicated by the *DR5:VENUS-NLS* reporter, there is an increase in auxin itself. Interestingly, the R2D2 data suggest that the greatest fold change in auxin concentration occurred in the endodermal cells in positions 2 to 6 (1 being closest to the QC), corresponding to the immediate vicinity of the dead vascular stem cells (Fig. 2*D*).

Despite only a minor difference in root length (*SI Appendix*, Fig. S2*B*), BLM treatment of auxin receptor mutants *tir1-1* and *tir1-1afb2-3* revealed a significantly lower recovery rate in both mutants (67% and 54%, respectively) compared with wild type (92%), suggesting that receptor-mediated auxin perception is essential during BLM recovery.

ERF115 Activation and Auxin Signaling Are Codependent. The observed accumulation of auxin around the dead cells, reminiscent of the *ERF115* expression pattern, suggests that auxin might be a main trigger for *ERF115* induction following vascular cell death. A recent study has shown that methyl jasmonate (MeJA) and auxin work in synergy to induce *ERF115* in protoxylem and QC cells in a manner depending on the MeJA receptor CORONATINE INSENSITIVE 1 (COI1) (39). Independently, it has been reported that *ERF115* expression can be induced by hydrogen peroxide (H_2O_2) (40). We observed that in the absence of BLM, *ERF115* expression induced by the auxin indole-3-acetic acid (IAA), a combination of IAA and MeJA, or H_2O_2 treatment remained restricted to the two protoxylem strands and QC cells (*SI Appendix*, Fig. S3 *A–C*). These results suggest that auxin, MeJA, or H_2O_2 by itself is not sufficient to induce *ERF115* as broadly as after cell death, which likely also requires an as-yet unidentified signal originating from the dead cells. Although we have confirmed that the protoxylem induction pattern depends on the COI1 receptor, BLM-induced *ERF115* expression does not, as the *ERF115:GFP-GUS* reporter was equally induced around the cell death zone in the wild type and *coi1-2* receptor mutant background (*SI Appendix*, Fig. S3*B*). This result indicates that COI1-mediated JA perception is not necessary for *ERF115* expression on BLM-induced cell death.

In contrast to MeJA, auxin appears to be essential for both the *ERF115* expression pattern and the stem cell recovery process. BLM recovery on medium with kynurenine and yucasin, chemical inhibitors of auxin biosynthesis, caused a reduction in *ERF115* accumulation and interfered with the root tip regeneration process, resulting in collapsed meristems (Fig. 3 *A* and *B*). Inversely, recovery on medium with 1-naphthaleneacetic acid (NAA) caused a clear thickening of the vascular bundle along with a seemingly increased number of *ERF115*-expressing cells (Fig. 3*C*). Taken together, these results suggest that while auxin is not the main trigger of ERF115 following BLM-induced cell death, it is necessary to maintain *ERF115* expression once induced.

To investigate whether ERF115 in turn could be involved in the activation of auxin signaling, we introduced the *DR5:GFP* reporter into the *35S:ERF115-SRDX* background. In this background, following prior treatment for 24 h with BLM, the DR5:GFP signal was strongly reduced during the recovery on BLM-free medium (Fig. 3*D*) compared with that in wild type plants (Fig. 3*E*). Recovery on kynurenine and yucasin resulted in a similar absence of auxin signaling (Fig. 3*F*), suggesting that both ERF115 activity and auxin biosynthesis are necessary for the activation of auxin signaling during stem cell replenishment.

BLM-Induced Stem Cell Death Obstructs Auxin Transport, Causing Auxin Accumulation without Activating Auxin Biosynthesis. Since treatment with auxin biosynthetic inhibitors impaired DR5:GFP accumulation after BLM treatment and resulted in meristem collapse, we reasoned that auxin biosynthesis might be activated around the dead cells. It was previously shown that the auxin biosynthesis gene *YUCCA9* is rapidly induced on root tip excision (43). In contrast, the *YUC9:VENUS* reporter line revealed no apparent transcriptional induction after 24 h of BLM treatment or 24 h after recovery (Fig. 4*A*). Similarly, *TAA1*, a major auxin biosynthetic gene with expression in the SCN, was not induced, as revealed by the *TAA1:TAA1-GFP* reporter line (Fig. 4*B*).

Similarly, a transcriptome dataset obtained from BLM-treated root tips (Dataset S1) showed no significantly up-regulated transcripts associated with the auxin biosynthesis pathway (Fig. 4*C*). Furthermore, free and conjugated IAA levels in root tips did not change significantly after BLM treatment (Fig. 4*D*). This led us to hypothesize that the observed auxin accumulation might be sourced from already established centers of auxin biosynthesis. Interestingly, transcript levels for auxin transport genes *PIN1*, *PIN4*, and *LAX2* were significantly down-regulated following BLM treatment, pointing to altered auxin transport (Fig. 4*C*). Imaging of translational reporter lines for PIN efflux proteins revealed a general absence of PIN1 and PIN3 at the position of dead cells, with an additional 30% down-regulation of PIN1 along the entire meristem. The PIN4 signal also showed a 13% decrease; however, owing to the high variability in this specific reporter line, the difference was not significant (*SI Appendix*, Fig. S4 *A–D*). PIN2 remained largely unchanged (*SI Appendix*, Fig. S4*B*).

To test whether the disruption of PIN-mediated auxin transport routes caused by cell death could explain the auxin accumulation in the vasculature and endodermal cells, we used an in silico model of polar auxin transport. Ten individual cell death patterns inferred from confocal images of BLM-treated roots were mimicked in silico by removing all auxin flows into and from the dead cells (*SI Appendix*, Fig. S5*B*). The model parameters were also adjusted for PIN1 down-regulation. Accumulation of auxin above and around the dead cells was predicted by the computational model in all different cell death patterns. Interestingly, the exact pattern of auxin accumulation tended to differ slightly among varying cell death patterns (*SI Appendix*, Fig. S4). Averaging the data obtained from 10 simulated cell death patterns revealed the greatest auxin accumulation in the vasculature and endodermis (Fig. 4*E*). The fold changes in the predicted auxin concentrations were in striking agreement with the auxin accumulation data obtained from the in vivo R2D2 reporter line (Fig. 2 *C* and *D*).

To study the contribution of the down-regulation in PINs, we recalculated the steady-state solutions by assuming that PIN levels were unchanged. Interestingly, the pattern of auxin accumulation was very similar to that obtained by assuming PIN down-regulation, but the fold changes in auxin ratios were reduced (*SI Appendix*, Fig. S6 *A* and *B*). Our modeling results indicate that simply omitting the dead cells as components of auxin flux is sufficient to recreate the experimentally observed pattern of auxin accumulation. Down-regulation of PIN-mediated rootward auxin transport likely contributes to the increased intensity of auxin accumulation. Taken together, these results suggest that disruption of auxin transport is likely one of the major dynamics contributing to the auxin accumulation observed after stem cell death.

ERF115 Boosts the Ability of Auxin Accumulation to Grant Stem Cell Identity and Results in Abundant Formative Cell Divisions. To study the effect of ERF115 on auxin accumulation, seedlings were grown on medium supplemented with the polar auxin transport inhibitor *N*-1-naphthylphthalamic acid (NPA) and analyzed at 5 and 14 d after germination. In addition to the appearance of QC markers in the endodermis, germination on NPA was reported to cause the expansion of the columella fate domain along the root cap, as indicated by accumulation of starch granules (44). After 5 d of growth on NPA, expansion of the starch granule region was not changed in the *35S:ERF115-SRDX* plants compared with the wild type, but was greatly enhanced in the *35S:ERF115* plants (Fig. 5*A*). Specific expression of *ERF115* in the endodermis (*EN7:ERF115*) was sufficient to mimic this phenotype (Fig. 5*A* and *SI Appendix*, Fig. S7*A*), suggesting that ERF115 enhances the effect of auxin accumulation in the endodermis to induce stem cell divisions in the surrounding cell files. NPA treatment for 2 wk caused the formation of thick stubby roots in the *35S:ERF115* line (Fig. 5*D*) compared with the wild type (Fig. 5*C*). Images from transverse microtome sections revealed massive cell proliferation

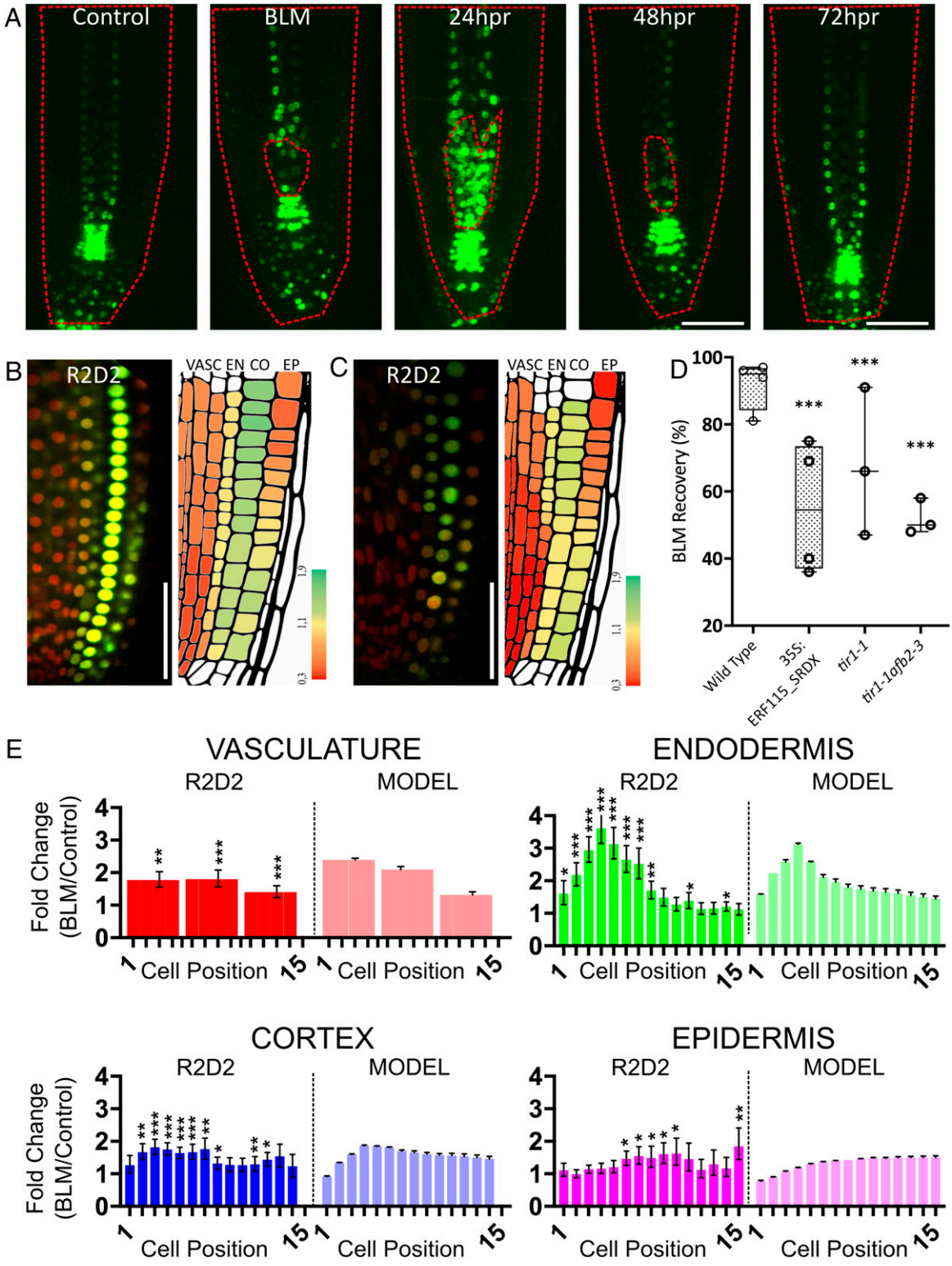

Fig. 2. (*A*) Confocal images of *DR5:Venus-NLS* under control conditions and during BLM recovery for indicated times. hpr, hours postrecovery. Images represent maximum intensity projections from 10 slices acquired at 1.5-μm intervals. Dashed red lines indicate the outline of the root and the region containing the dead cells, as inferred from propidium iodide staining (*SI Appendix*, Fig. S2*A*). (*B* and *C*) Confocal images of a R2D2 ratiometric auxin reporter line grown under control conditions (*B*) and after BLM treatment (*C*). Cartoons are representative images reconstructed from average R/G ratios calculated from 12 images. A higher red/green ratio corresponds to higher auxin levels. (Scale bars in *A* and *B*: 50 μm.) VASC, vasculature; EN, endodermis; CO, cortex; EP, epidermis. (*D*) BLM recovery percentages of wild-type, *35S:ERF115-SRDX*, *tir1-1*, and *tir1-1afb2-3* mutants. ***$P < 0.001$. (*E*) Side-by-side comparison of average fold changes in auxin concentrations as observed in vivo (R2D2) and predicted by the in silico model (MODEL). Error bars represent maximal errors calculated as described in *Materials and Methods*. Fold changes (BLM/control) in R/G ratios were obtained from R2D2 images according to the cell position in the respective tissues. Ratios from all cells within cell positions 1 to 5, 6 to 10, and 11 to 15 were averaged and plotted as three data points. *$P < 0.05$; **$P < 0.01$; ***$P < 0.001$.

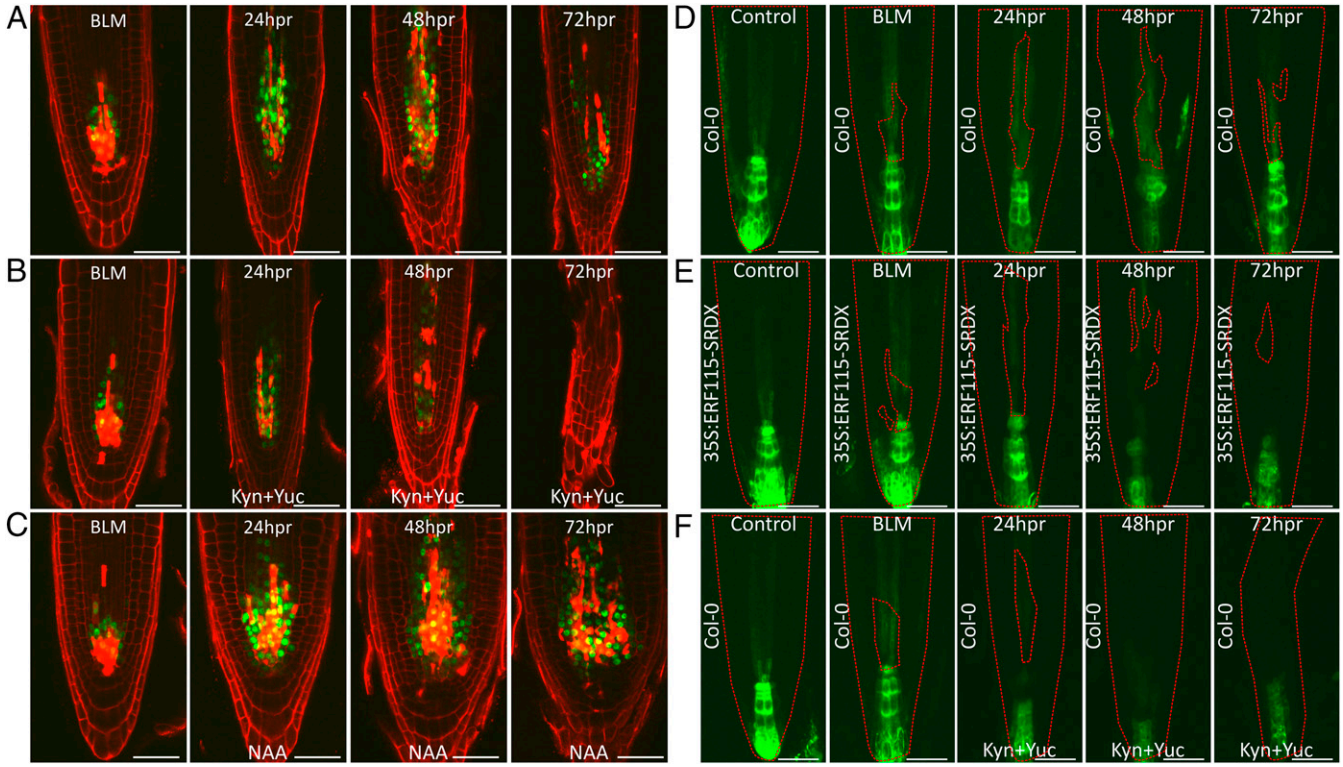

Fig. 3. Confocal images of *pERF115:GFP-GUS* (*A*–*C*) and *DR5:GFP* (*D*–*F*) seedlings in wild-type (*A*, *B*, *C*, *D*, and *F*) or *35S:ERF115-SRDX* (*E*) background treated for 24 h with BLM and recovered on normal medium supplemented with DMSO (*A*, *D*, and *E*), with auxin biosynthesis inhibitors kynurenine and yucasin (*B* and *F*) or with 1 μM NAA (*C*). Red dashed lines in *D*–*F* indicate the outline of the root and the region containing the dead stem cells as indicated by propidium iodide staining (*SI Appendix*, Fig. S3 *D*–*F*). (Scale bars: 50 μm.)

in the *35S:ERF115* line and to a lesser extent in the *EN7:ERF115* line compared with the wild type (Fig. 5*B*). In contrast, the *35S:ERF115-SRDX* line responded to NPA treatment similarly to wild type (Fig. 5 *A* and *B*). These results suggest that *ERF115* expression increases the number of formative divisions triggered as a result of auxin accumulation. *ERF115* expression in the endodermis is sufficient to enhance its ability to organize stem cell fates in the surrounding cell files on auxin accumulation (Fig. 5 *A* and *B*). The similar response to NPA treatment in the *35S:ERF115-SRDX* line and wild-type plants might indicate that ERF115 signaling is not required for the lateral root cap cells to acquire starch granules.

To understand how ERF115 might regulate the response to auxin accumulation caused by DNA damage-induced cell death, we looked at the components of auxin signaling differentially regulated in our BLM transcriptome dataset. Among these were several members of the *AUX/IAA* (*IAA1*, *5*, *13*, *19*, *20*, *29*, *33*) and *AUXIN RESPONSE FACTOR* (*ARF3*, *5*, *8*) gene families that regulate TIR1/AFB receptor- mediated auxin signaling (Fig. 6 *A* and *B*) (11). Notably, *ARF5/MP* was the only *ARF* significantly induced by both BLM treatment (fold change = 1.62; FDR = 1,44e-02) and *ERF115* overexpression (fold change = 1.53; P = 4,5e-03) (Dataset S1). Bioinformatic analysis based on previously published DNA affinity purification sequencing (DAP-seq) data (45) suggested that the upstream genomic regions of BLM-induced and -repressed genes (Dataset S1) are significantly enriched and depleted for ARF5/MP-binding regions, respectively (*SI Appendix*, Table S3). Therefore, we reasoned that the activation of auxin signaling on auxin accumulation after BLM treatment and during recovery might be regulated, at least in part, by ARF5/MP. The DAP-seq data indicated two general AP2/ERF-binding regions (−2,753 to −2,543 bp and −2,293 to −2,093 bp upstream of the *ARF5/MP* start codon) that overlapped with a DNase hypersensitive (DHS) site (−2,793 to −2,643 bp). This DHS region also coincided with one of two putative ERF115-binding regions (−2,950 to −2,487 bp) annotated by TChAP-seq (Fig. 6*C*) (45, 46).

Next, we scanned the *ARF5/MP* upstream region with the position weight matrix for ERF115 (*SI Appendix*, Fig. S7*B*) according to O'Malley et al. (47), which revealed two partially overlapping ERF115-binding regions at −2,753 to −2,737 bp (P = 3.47e-05) and −2,745 to −2,729 bp (P = 8.73e-05) upstream (Fig. 6*D*). These data suggested that *ARF5/MP* might be a direct transcriptional target of ERF115; therefore, we asked whether the absence of auxin signaling activation in BLM-treated *35S:ERF115-SRDX* seedlings could be explained by a reduction in *ARF5/MP* levels. qRT-PCR analysis revealed lower *ARF5/MP* expression under control conditions in *35S:ERF115-SRDX* seedlings, and no induction was observed on BLM treatment (Fig. 6*D*). Confocal imaging of an *MP:MP-GFP* translational reporter revealed greatly enhanced ARF5/MP accumulation in the *35S:ERF115* background under control conditions, after BLM treatment, and after 24 h of recovery. Reciprocally, the MP:MP-GFP signal was reduced in the *35S:ERF115-SRDX* line (Fig. 6*E*). Furthermore, there was a significant decrease in NPA-induced starch granule accumulation among seedlings hemizygous for the *mpB4149* mutation compared with wild-type seedlings, pointing to the need for MP/ARF5 in the response to auxin accumulation (Fig. 6*F*). Taken together, these results suggest that the activation of auxin signaling on BLM-induced cell death might be regulated, at least in part, by ARF5/MP in an ERF115-dependent manner.

Discussion

ERF115 has previously been identified as a rate-limiting factor for the proliferation of QC stem cells, which are marked by an auxin maximum (36). In addition, ERF115 activity was found to

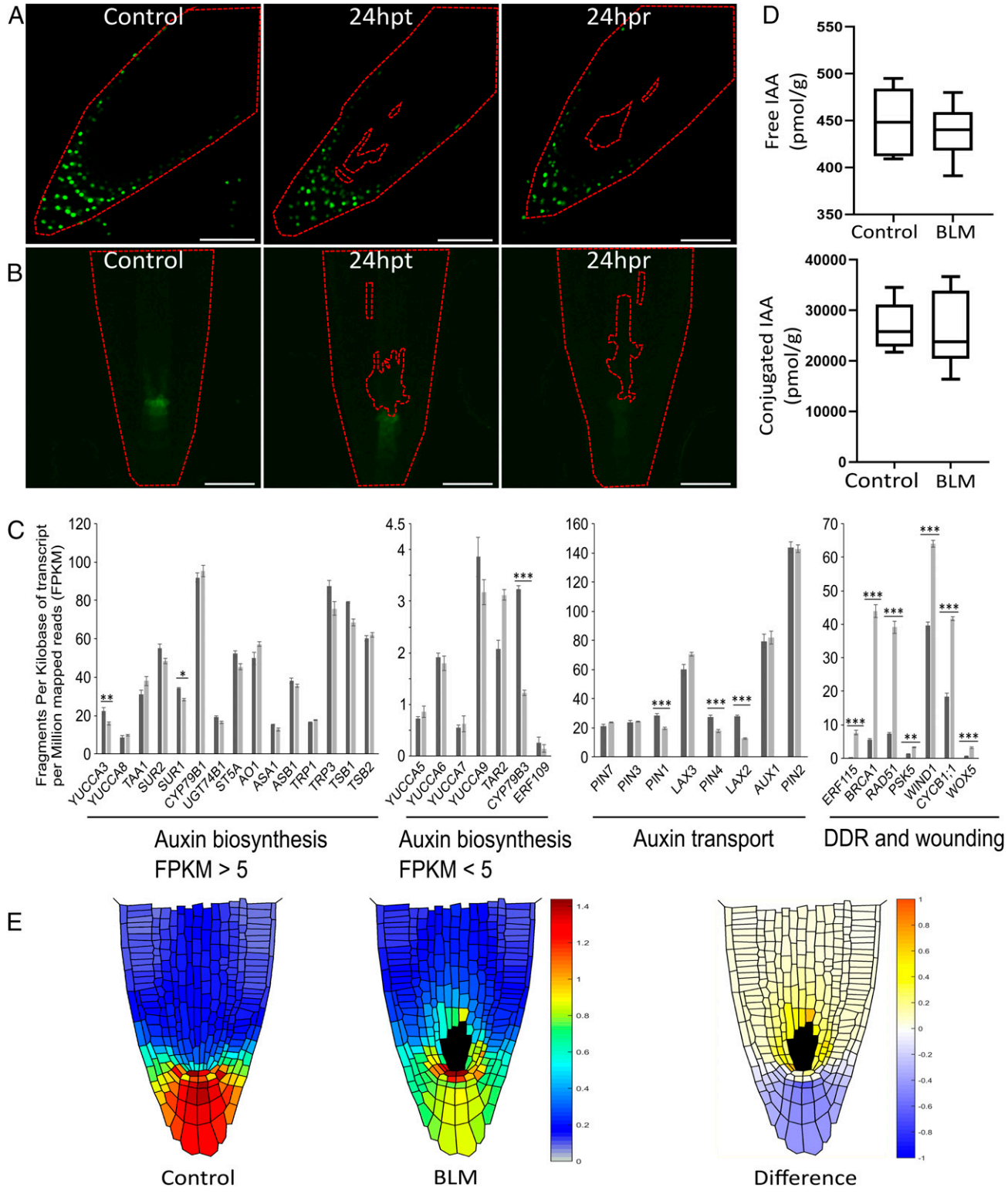

Fig. 4. (*A* and *B*) Confocal images of *YUC9:VENUS* (*A*) and *TAA1:TAA1-GFP* (*B*) seedlings before and after BLM treatment and indicated times of recovery. The red dashed line outlines the root and the location of dead cells as inferred by propidium iodide staining. hpt, hours posttreatment; hpr, hours postrecovery. (Scale bars: 50 μm.) (*C*) Transcriptional changes in auxin biosynthesis and transport genes and genes involved in the DNA damage response (DDR) and wounding, revealed by RNA-seq from BLM-treated root tips. *FDR < 0.05; **FDR < 0.01; ***FDR < 0.001. (*D*) Free and conjugated IAA concentrations before and after BLM treatment. (*E*) Auxin distributions obtained from an in silico model of polar auxin transport before and after BLM-induced stem cell death. The BLM picture represents the average obtained from simulation of 10 real-life cell death patterns. The plot represents the average fold changes in auxin concentrations per tissue against distance from the QC.

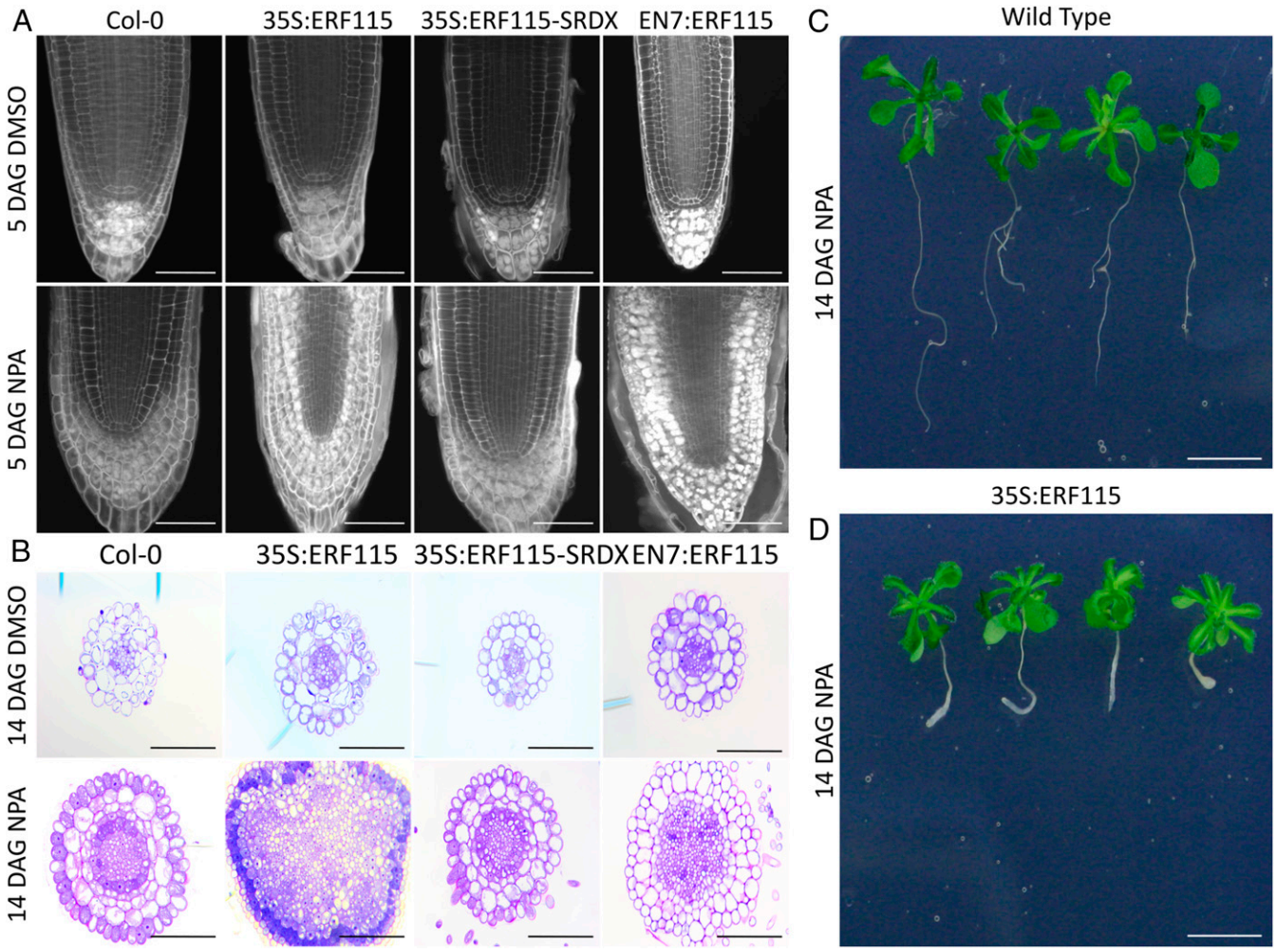

Fig. 5. (*A*) Confocal images of pseudo-Schiff-stained Col-0, *35S:ERF115*, *35S:ERF115-SRDX*, and *pEN7:ERF115* seedlings grown for 5 d on DMSO or 10 μM NPA. (*B*) Cross-sectional images of Col-0, *35S:ERF115*, *35S:ERF115-SRDX*, and *EN7:ERF115* seedlings grown for 14 d on DMSO or 10 μM NPA. Sections correspond to the region 650 to 750 μm from the root tip. (*C* and *D*) Col-0 (*C*) and *35S:ERF115* (*D*) seedlings grown on 10 μM NPA for 14 d. (Scale bars: *A* and *B*, 100 μm; *C* and *D*, 1 cm.) DAG, days after germination.

be induced within the root meristem on wounding by tip excision or DNA damage and to be essential for the root regeneration process following such wounding (37). Here we report that induction of *ERF115* by cell death acts as a modulator within regions of developmental or wound-induced auxin accumulation to confer the formative capacity necessary for regeneration.

Using a lineage tracking tool, we showed that the replenishment of vascular stem cells that have undergone DNA damage-induced cell death is driven predominantly by endodermal cells undergoing formative divisions. However, since the *SCR* promoter used in the lineage tracking line also labels the QC cells, a contribution from the QC cells cannot be excluded. In the *ERF115-SRDX* dominant-negative background, the CFP-labeled endodermis/cortex cell files were zipped together following collapse of the damaged vascular cells. Furthermore, suppression of ERF115 activity specifically in the endodermis impaired recovery, suggesting that endodermal ERF115-dependent formative divisions are essential for successful replenishment of vascular cells. This regenerative program is likely linked to the type of cell death. With the vascular stem cells characteristically more sensitive to DNA damage, resulting in severe vascular cell death, endodermal cells appear to be the most likely tissue to initiate the recovery of vascular cell files. In contrast, Efroni et al. (23) reported that on removal of the SCN by root tip excision, an inside-out mode of regeneration occurs, in which the new SCN is formed mainly by the surviving vascular cells. In this mode of regeneration, the endodermal cells contribute mostly to the epidermis and lateral root cap. Similarly, in the case of targeted cell elimination by laser ablation, the dead cells were shown to be replaced exclusively by their inward neighbors (38). Taken together, these findings suggest that the mode of regeneration can adapt to meet the specific regenerative requirements created by different types and intensities of injury.

It has been previously shown that spatially altering auxin maxima through the application of polar auxin transport inhibitors triggers the QC fate gain in the endodermis and in turn creates stem cell patterns in the surrounding cell layers (44, 49). Based on these findings, a model has been proposed stating that meristematic endodermal cells are competent to become QC stem cells, and that the location of the actual QC is determined by that of the auxin maximum. In turn, the QC cells maintain a functional SCN around them that is essential for indeterminate growth. Our work indicates that the model proposed by Sabatini et al. (44, 49) can be extended from developmental conditions to regeneration processes. At least in the context of BLM-induced vascular cell death, we showed that auxin accumulates in the

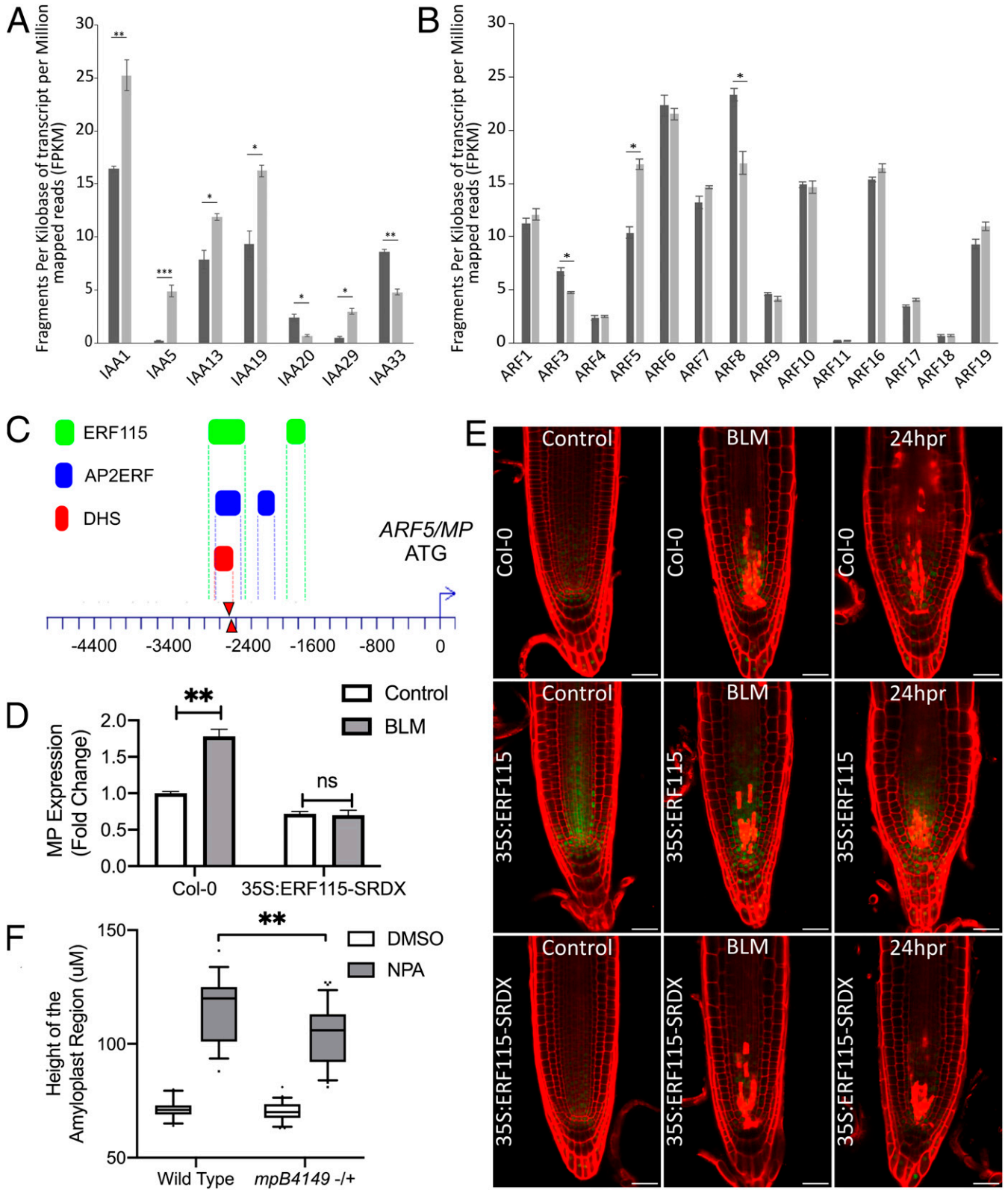

Fig. 6. (*A* and *B*) Fragments per kilobase of transcript per million reads (FPKM) of only differentially expressed *AUX/IAA* genes (*A*) and all *ARF* genes (*B*) obtained from RNA-seq transcriptome of BLM- vs. mock-treated seedlings. $*P < 0.01$; $**P < 0.01$; $***P < 0.001$. (*C*) Putative AP2/ERF transcription factor binding regions (blue) according to O'Malley et al. (47), DNAse I hypersensitive site (DHS, red) according to Sulliven et al. (48), and putative ERF115-binding regions (green) according to Heyman et al. (46). (*D*) Fold changes in expression of *MP* with or without BLM treatment in Col-0 and *35S:ERF115-SRDX* as indicated by qRT-PCR. (*E*) *MP:MP-GFP* reporter line in Col-0, *35S:ERF115*, and *35S:ERF115-SRDX* background before and after BLM treatment or 24 h post recovery (hpr). (Scale bars: 50 μm.) (*F*) Starch granule area quantification obtained from a segregating population of *mpB4149* mutants. Homozygous mutant seedlings were not included in the analysis due to lack of a root.

vascular and endodermal cells after BLM treatment. The auxin receptor mutants *tir1-1* and *tir1-1afb2-3* have significantly decreased BLM recovery rates, highlighting the importance of receptor-mediated perception of the auxin accumulation following BLM treatment. This auxin accumulation is correlated with ERF115-dependent ectopic expression of *WOX5:GFP* predominantly in the endodermal cell file, but not of *QC25:GUS*, suggesting at least a partial gain of QC cell identity of the endodermal cells positioned directly next to the dead vascular cells. Reciprocally, mimicking auxin accumulation in undamaged roots by NPA treatment in combination with ubiquitous or endodermis-specific *ERF115* overexpression results in extensive formative divisions in the vasculature and ground tissue and expansion of the columella cell fate region.

These observations suggest that the ectopic (partial) gain of the QC fate by the endodermis observed during BLM recovery is a direct result of the combined ERF115 activation and auxin accumulation in the endodermis. This in turn confers a formative capacity to the endodermis that is necessary for successful regeneration from DNA damage-induced stem cell death. The accumulation of auxin in the endodermis is likely temporary, since the regeneration process reestablishes the auxin flow. This temporary auxin accumulation is insufficient for the full realization of QC attributes, such as the ectopic formation of columella starch granules in the epidermis observed after continuous auxin accumulation by NPA treatment.

Activation of auxin biosynthesis during the recovery from root tip excision and de novo root organogenesis has been reported previously (43, 50, 51). However, BLM-induced stem cell death does not cause up-regulation of auxin biosynthetic genes, as suggested by reporter lines and transcriptome data. Nevertheless, chemical inhibition of auxin biosynthesis impairs the accumulation of auxin and *ERF115* expression after cell death. This suggests that preestablished sites of auxin biosynthesis likely provide the auxin that accumulates around the dead cells. Therefore, we reason that a perturbed polar auxin transport might be responsible for the observed auxin accumulation. In line with earlier reports (10), an obstruction in auxin transport was suggested by the disappearance of PIN1 and PIN3 at the positions of dead cells following laser ablation of QC cells or root tip excision. Indeed, simulating stem cell death in an established in silico model of auxin transport predicted an accumulation of auxin around the dead cells, in line with the observed in vivo data. Taken together, these data suggest that on DNA damage, the dead stem cells might obstruct the normal auxin flow, causing auxin accumulation in the surrounding tissues.

This raises a very interesting question: how does the root know when to activate auxin biosynthesis? We hypothesize that the key difference might be the degree to which auxin transport is blocked. Throughout development, organ formation occurs at sites of persistent auxin accumulation formed by polar auxin transport, such as shoot primordia, floral meristems, and lateral roots (52–56). In this hypothesis, auxin biosynthesis is induced only in the case of de novo organ formation, such as de novo root regeneration from an excised root or cotyledon. On root tip excision, the flow of auxin through the vasculature is abruptly and completely blocked, which causes auxin to accumulate persistently at the terminal point of the remaining vasculature. This abrupt accumulation could be the cue for de novo generation of the new tip by reactivation of local auxin biosynthesis. This would lead to determination of a new maximum and regeneration of the root tip, the major structure redirecting auxin flow upward to the epidermis and then back into the meristem. In contrast, DNA damage-induced stem cell death causes a partial and gradual obstruction of auxin transport as stem cells die in a progressive manner (Movie S2), with accumulation below the threshold for triggering de novo biosynthesis. As long as the auxin accumulation intensity is below the necessary threshold, de novo creation of a stem cell niche and root tip is not triggered; instead, replenishment from the surviving nearby tissues by formative divisions is sufficient to restore the auxin flux.

To understand how ERF115 might regulate the auxin response, we analyzed the expression of core regulators of auxin signaling on BLM treatment. Interestingly, the only ARF induced by BLM treatment was ARF5/MP, a major regulator of embryonic polarity, shoot apical meristem primordia, lateral organ, and vascular tissue development (13–17, 52, 53). BLM-induced genes identified via RNA-seq were significantly enriched in ARF5/MP-binding regions, suggesting that ARF5/MP might play an essential role in the activation of auxin signaling. Moreover, expression of *ARF5/MP* on BLM treatment was dependent on ERF115 activity, and the promoter region of *ARF5/MP* contains a putative ERF115-binding region according to two independent datasets (45, 46). These data suggest that ERF115 is a wound-inducible modulator of auxin signaling, possibly by acting upstream of ARF5/MP, feeding wounding input into auxin-mediated developmental processes, such as tissue patterning and organ formation. Since our data also show that *ERF115* expression is dependent on the presence of auxin, cell death-induced auxin accumulation by obstruction of polar transport simultaneously maintains *ERF115* expression and induces regenerative divisions in a synergistic manner.

Materials and Methods

Plant Materials and Growth Conditions. *pSCR:CRE-GR p35S loxp-tOCS-loxp-CFP* seeds were kindly provided by Kenneth Birnbaum, New York University (23). *DR5:GFP*, *PIN1:PIN1-GFP*, *PIN2:PIN2-GFP*, and *PIN3:PIN3-GFP* reporter lines were obtained from the *Arabidopsis* Biological Resource Center. The R2D2 reporter line has been described previously (42). For the *EN7:ERF115* and *EN7:ERF115-SRDX* lines, the genomic *ERF115* sequence with or without an SRDX domain was cloned with the *EN7* promoter into the pB7m24GW,3 destination vector and selected for Basta resistance. The *WOX5*-NLS/GFP-GUS and ERF115:NLS/GFP-GUS reporter lines have been described previously (36, 37). Plants were grown under a long-day regime (16-h light/8-h dark) on agar-solidified culture medium (Murashige and Skoog medium, 10 g/L saccharose, 4.3 g/L 2-(*N*-morpholino) ethanesulfonic acid, and 0.8% plant tissue culture agar) at 21 °C.

Study protocols are described more detail in *SI Appendix*.

Data Availability Statement. RNA-seq data have been deposited in the Gene Expression Omnibus (GEO) database, https://www.ncbi.nlm.nih.gov/geo (accession no. GSE139715) (57). All seeds and vectors are freely available from the corresponding author on request. Protocol details are described in the *SI Appendix*.

ACKNOWLEDGMENTS. We thank Annick Bleys for help with manuscript preparation, Sevgi Öden and Tim Willems for technical assistance, and Veronique Storme for biostatistical analysis and guidance. This work was supported by a grant from the Research Foundation-Flanders (G007218N). J.H. is indebted to the Research Foundation-Flanders for a postdoctoral fellowship. Mathematical modeling was supported by the Russian Science Foundation (18-74-10008), and sequence analysis was supported by the Ministry of Science and Higher Education of the Russian Federation (0324–2019-0040-**C**-01). RNA-seq library preparation and sequencing were performed by the VIB Nucleomics Core (www.nucleomics.be).

1. E. Aichinger, N. Kornet, T. Friedrich, T. Laux, Plant stem cell niches. *Annu. Rev. Plant Biol.* **63**, 615–636 (2012).
2. L. Pi *et al.*, Organizer-derived WOX5 signal maintains root columella stem cells through chromatin-mediated repression of *CDF4* expression. *Dev. Cell* **33**, 576–588 (2015).
3. T. Bennett, B. Scheres, Root development—two meristems for the price of one? *Curr. Top. Dev. Biol.* **91**, 67–102 (2010).
4. C. M. Ha, J. H. Jun, J. C. Fletcher, Shoot apical meristem form and function. *Curr. Top. Dev. Biol.* **91**, 103–140 (2010).
5. L. Gutierrez *et al.*, Phenotypic plasticity of adventitious rooting in Arabidopsis is controlled by complex regulation of AUXIN RESPONSE FACTOR transcripts and microRNA abundance. *Plant Cell* **21**, 3119–3132 (2009).
6. M. Asahina *et al.*, Spatially selective hormonal control of RAP2.6L and ANAC071 transcription factors involved in tissue reunion in Arabidopsis. *Proc. Natl. Acad. Sci. U.S.A.* **108**, 16128–16132 (2011).
7. C. W. Melnyk, Connecting the plant vasculature to friend or foe. *New Phytol.* **213**, 1611–1617 (2017).

8. L. Xu, De novo root regeneration from leaf explants: Wounding, auxin, and cell fate transition. *Curr. Opin. Plant Biol.* **41**, 39–45 (2018).
9. M. Ikeuchi, Y. Ogawa, A. Iwase, K. Sugimoto, Plant regeneration: Cellular origins and molecular mechanisms. *Development* **143**, 1442–1451 (2016).
10. G. Sena, X. Wang, H. Y. Liu, H. Hofhuis, K. D. Birnbaum, Organ regeneration does not require a functional stem cell niche in plants. *Nature* **457**, 1150–1153 (2009).
11. M. Lavy, M. Estelle, Mechanisms of auxin signaling. *Development* **143**, 3226–3229 (2016).
12. B. De Rybel *et al*., A bHLH complex controls embryonic vascular tissue establishment and indeterminate growth in Arabidopsis. *Dev. Cell* **24**, 426–437 (2013).
13. L. Luo, J. Zeng, H. Wu, Z. Tian, Z. Zhao, A molecular framework for auxin-controlled homeostasis of shoot stem cells in Arabidopsis. *Mol. Plant* **11**, 899–913 (2018).
14. G. K. Przemeck, J. Mattsson, C. S. Hardtke, Z. R. Sung, T. Berleth, Studies on the role of the Arabidopsis gene MONOPTEROS in vascular development and plant cell axialization. *Planta* **200**, 229–237 (1996).
15. T. B. G. Jürgens, The role of the monopteros gene in organising the basal body region of the Arabidopsis embryo. *Development* **118**, 575–587 (1993).
16. T. Hamann, E. Benkova, I. Bäurle, M. Kientz, G. Jürgens, The Arabidopsis BODENLOS gene encodes an auxin response protein inhibiting MONOPTEROS-mediated embryo patterning. *Genes Dev.* **16**, 1610–1615 (2002).
17. I. De Smet *et al*., Bimodular auxin response controls organogenesis in Arabidopsis. *Proc. Natl. Acad. Sci. U.S.A.* **107**, 2705–2710 (2010).
18. S. M. Rozov, A. A. Zagorskaya, E. V. Deineko, V. K. Shumny, Auxin: Regulation and its modulation pathways. *Biol. Bull. Rev.* **3**, 423–430 (2013).
19. S. V. Petersson *et al*., An auxin gradient and maximum in the Arabidopsis root apex shown by high-resolution cell-specific analysis of IAA distribution and synthesis. *Plant Cell* **21**, 1659–1668 (2009).
20. H. Tian, T. Niu, Q. Yu, T. Quan, Z. Ding, Auxin gradient is crucial for the maintenance of root distal stem cell identity in Arabidopsis. *Plant Signal. Behav.* **8**, e26429 (2013).
21. I. Blilou *et al*., The PIN auxin efflux facilitator network controls growth and patterning in Arabidopsis roots. *Nature* **433**, 39–44 (2005).
22. Y. Tao *et al*., Rapid synthesis of auxin via a new tryptophan-dependent pathway is required for shade avoidance in plants. *Cell* **133**, 164–176 (2008).
23. I. Efroni *et al*., Root regeneration triggers an embryo-like sequence guided by hormonal interactions. *Cell* **165**, 1721–1733 (2016).
24. I. Ottenschläger *et al*., Gravity-regulated differential auxin transport from columella to lateral root cap cells. *Proc. Natl. Acad. Sci. U.S.A.* **100**, 2987–2991 (2003).
25. R. A. R. Machado *et al*., Auxin is rapidly induced by herbivore attack and regulates a subset of systemic, jasmonate-dependent defenses. *Plant Physiol.* **172**, 521–532 (2016).
26. K. Kazan, Auxin and the integration of environmental signals into plant root development. *Ann. Bot.* **112**, 1655–1665 (2013).
27. S. Mroue, A. Simeunovic, H. S. Robert, Auxin production as an integrator of environmental cues for developmental growth regulation. *J. Exp. Bot.* **69**, 201–212 (2018).
28. J. Wisniewska *et al*., Polar PIN localization directs auxin flow in plants. *Science* **312**, 883 (2006).
29. R. Benjamins *et al*., PPP1, a plant-specific regulator of transcription controls Arabidopsis development and PIN expression. *Sci. Rep.* **6**, 32196 (2016).
30. V. V. Mironova *et al*., Combined in silico/in vivo analysis of mechanisms providing for root apical meristem self-organization and maintenance. *Ann. Bot.* **110**, 349–360 (2012).
31. R. Benjamins, B. Scheres, Auxin: The looping star in plant development. *Annu. Rev. Plant Biol.* **59**, 443–465 (2008).
32. O. Leyser, C. Sedwick, Ottoline Leyser: The beauty of plant genetics. Interviewed by Caitlin Sedwick. *J. Cell Biol.* **204**, 284–285 (2014).
33. M. Aida *et al*., The PLETHORA genes mediate patterning of the Arabidopsis root stem cell niche. *Cell* **119**, 109–120 (2004).
34. G. Vert, J. Chory, Crosstalk in cellular signaling: Background noise or the real thing? *Dev. Cell* **21**, 985–991 (2011).
35. S. Depuydt, C. S. Hardtke, Hormone signalling crosstalk in plant growth regulation. *Curr. Biol.* **21**, R365–R373 (2011).
36. J. Heyman *et al*., ERF115 controls root quiescent center cell division and stem cell replenishment. *Science* **342**, 860–863 (2013).
37. J. Heyman *et al*., The heterodimeric transcription factor complex ERF115-PAT1 grants regeneration competence. *Nat. Plants* **2**, 16165 (2016).
38. P. Marhava *et al*., Re-activation of stem cell pathways for pattern restoration in plant wound healing. *Cell* **177**, 957–969 e13 (2019).
39. W. Zhou *et al*., A jasmonate signaling network activates root stem cells and promotes regeneration. *Cell* **177**, 942–956 e14 (2019).
40. X. Kong *et al*., PHB3 maintains root stem cell niche identity through ROS-responsive AP2/ERF transcription factors in Arabidopsis. *Cell Rep.* **22**, 1350–1363 (2018).
41. R. A. Johnson *et al*., SUPPRESSOR OF GAMMA RESPONSE1 links DNA damage response to organ regeneration. *Plant Physiol.* **176**, 1665–1675 (2018).
42. C.-Y. Liao *et al*., Reporters for sensitive and quantitative measurement of auxin response. *Nat. Methods* **12**, 207–210, 2, 210 (2015).
43. D. Xu *et al*., YUCCA9-mediated auxin biosynthesis and polar auxin transport synergistically regulate regeneration of root systems following root cutting. *Plant Cell Physiol.* **58**, 1710–1723 (2017).
44. S. Sabatini *et al*., An auxin-dependent distal organizer of pattern and polarity in the Arabidopsis root. *Cell* **99**, 463–472 (1999).
45. A. Bartlett *et al*., Mapping genome-wide transcription-factor binding sites using DAP-seq. *Nat. Protoc.* **12**, 1659–1672 (2017).
46. J. Heyman *et al*., ERF115 controls root quiescent center cell division and stem cell replenishment. *Science* **342**, 860–863 (2013).
47. R. C. O'Malley *et al*., Cistrome and epicistrome features shape the regulatory DNA landscape. *Cell* **165**, 1280–1292 (2016).
48. A. M. Sullivan *et al*., Mapping and dynamics of regulatory DNA and transcription factor networks in A. thaliana. *Cell Rep.* **8**, 2015–2030 (2014).
49. S. Sabatini, R. Heidstra, M. Wildwater, B. Scheres, SCARECROW is involved in positioning the stem cell niche in the Arabidopsis root meristem. *Genes Dev.* **17**, 354–358 (2003).
50. G. Zhang *et al*., Jasmonate-mediated wound signalling promotes plant regeneration. *Nat. Plants* **5**, 491–497 (2019).
51. M. Ikeuchi *et al*., Wounding triggers callus formation via dynamic hormonal and transcriptional changes. *Plant Physiol.* **175**, 1158–1174 (2017).
52. N. Bhatia *et al*., Auxin acts through MONOPTEROS to regulate plant cell polarity and pattern phyllotaxis. *Curr. Biol.* **26**, 3202–3208 (2016).
53. N. S. Carey, N. T. Krogan, The role of AUXIN RESPONSE FACTORs in the development and differential growth of inflorescence stems. *Plant Signal. Behav.* **12**, e1307492 (2017).
54. E. Benková *et al*., Local, efflux-dependent auxin gradients as a common module for plant organ formation. *Cell* **115**, 591–602 (2003).
55. S. Stoma *et al*., Flux-based transport enhancement as a plausible unifying mechanism for auxin transport in meristem development. *PLOS Comput. Biol.* **4**, e1000207 (2008).
56. E. M. Bayer *et al*., Integration of transport-based models for phyllotaxis and midvein formation. *Genes Dev.* **23**, 373–384 (2009).
57. B. Canher, T. Eekhout, L. De Veylder, Data from "Rocks in the Auxin Stream: Wound induced auxin accumulation and ERF115 expression synergistically drive stem cell regeneration." NCBI Gene Expression Omnibus. https://www.ncbi.nlm.nih.gov/geo/query/acc.cgi?acc=GSE139715. Deposited 31 October 2019.